# Temperature-dependent Raman scattering studies in nanocrystalline silicon and finite-size effects

Puspashree Mishra* and K. P. Jain
*Department of Physics, Indian Institute of Technology, New Delhi 110016, India*
(Received 12 November 1999; revised manuscript received 17 May 2000)

A comparative study of the temperature-dependent Raman scattering of nanocrystalline and bulk silicon is presented. The nanocrystalline silicon samples were made by a cw laser annealing process, and the characteristic dimensions were determined with a phenomenological phonon confinement model. Experimental results indicate a higher degree of anharmonicity in nanocrystals compared to that in the bulk. The anharmonic constants are found to be highly size dependent and increase greatly with decreasing dimensions. The phonon lifetimes have two contributions, one temperature dependent and the other temperature independent, both decreasing rapidly with decreasing nanocrystal size. The temperature-dependent term $\tau_0$ is important for larger nanocrystals, while the temperature-independent term $\tau_1$ becomes dominant for nanocrystals of sizes less than 4 nm.

## I. INTRODUCTION

The experimental and theoretical study of semiconductor nanocrystallites[1,2] has generated tremendous technological and scientific interest recently due to the unique electronic and optical properties and exhibition of new quantum phenomena. The recent discovery of strong room-temperature photoluminescence from silicon nanocrystals fabricated by different methods is an extremely important scientific breakthrough with enormous technological implications, thus attracting much attention from a fundamental physics viewpoint and because of the potential applications in optical devices.[3,4]

The crystalline, amorphous, or nanocrystalline nature of any material can be ascertained by studying the first-order Raman spectra. Confinement or localization of phonons in finite-dimension nanocrystals introduces changes in the vibrational properties including a shift in phonon frequency and changes in the linewidth and asymmetry. These changes are functions of the dimension of the nanocrystal. The characteristic dimension of nanocrystals can be ascertained by analyzing the change in the line shape of the first-order Raman spectrum on the basis of a phenomenological model.[5,6]

Furthermore, the vibrational properties of semiconductors are also strongly influenced by temperature. An increase in temperature introduces perturbations in the harmonic potential term, which changes the vibrational properties. Optical phonons decay into two or more low-energy phonons due to anharmonic processes, which decreases their lifetimes. It is also pointed out that the carrier relaxation rate[7,8] is, in general, not dominated by emission, but is frequently dominated by the decay of strongly interacting optical phonons into weakly interacting acoustic phonons.

The temperature dependence of the Raman spectra of crystalline silicon has been studied by many authors.[9–11] They have studied both the line center and linewidth variations with temperature due to the presence of anharmonicity in the vibrational potential energy. The Klemens[10] model assumes that the contribution to the linewidth arises only from the decay of the optical phonon into two acoustic phonons of the same frequency and opposite momentum. Hart *et al.*[11] were able to show that their data for the damping constant can be fitted satisfactorily by the cubic anharmonic model of Klemens[10] if the zero-temperature value of the damping constant is properly chosen. Balkanski, Wallis, and Haro[9] calculated the change in linewidth and line center for the first-order LO phonon mode in silicon using cubic and quartic anharmonicity and found good agreement between theory and experiment.

Changes in the linewidth of the phonon in Raman and infrared spectra can be used as an indirect measurement for estimating the lifetime of strongly interacting optical phonons. A more direct measurement for estimating the lifetime of the optical phonons in the time domain, such as time-resolved spontaneous Raman scattering (TRSRS), can provide a detailed picture of the dephasing of molecular vibrations. However, important information concerning the phonon relaxation process can be obtained from an analysis of the broadening of Raman spectra, which is inversely related to the lifetime of the phonon.

Raman scattering in nanocrystalline semiconductors has been studied extensively.[12–16] However, very few experiments have been carried out to investigate the temperature dependence in nanocrystals. Finite-size effects in nanocrystals are expected to modify the anharmonicity and the phonon decay times. Richter *et al.*[5] presented the variation of the linewidth of silicon microcrystals of large dimensions and found an increase in the decay rate of optical phonons in the microcrystals compared to the bulk. Tanaka *et al.*[17] investigated the variation of the linewidth of CdSe microcrystals and arrived at a similar conclusion as that of Richter *et al.*[5] There have been, however, no reports of variations of the peak positions with temperature in nanocrystals. Further, the anharmonicity in very small nanocrystals has not been investigated as yet.

The purpose of this paper is to examine the effects of confinement and temperature-induced changes on vibrational states of silicon nanostructures using Raman spectroscopy. Silicon nanostructures used in the present study were prepared by cw laser annealing of hydrogenated amorphous silicon. The average dimension of nanocrystals was determined using the phonon confinement model. The contributions

 

from the amorphous background and strain have been determined to ascertain the proper line shapes. Measurements of the Raman scattering spectra for different dimension nanocrystals are presented in the temperature range 10–300 K. The results are analyzed in terms of anharmonic and finite-size effects. It is found that the anharmonicities for nanocrystals are larger than those in the bulk and increase asymptotically with decreasing dimensions. Furthermore, phonon lifetimes are influenced by both thermal and finite-size effects, the latter predominating for very small nanocrystals.

## II. EXPERIMENTAL PROCEDURE

Raman scattering experiments were performed in a backscattering geometry configuration at different temperatures by employing the 514.5-nm wavelength of the argon-ion laser, the RAMANOR double monochromator, and photon counting electronics. The Si nanocrystals used for this experiment were fabricated by cw laser annealing of *a*-Si:H samples of thicknesses 1100 and 5000 Å grown on quartz substrates. The *a*-Si:H samples were fabricated using the glow discharge method with the quartz substrates maintained at 250 °C. The hydrogen concentration in the film was roughly 8%. Controlled cw laser annealing of the *a*-Si:H samples on diffraction-limited spots of 40 $\mu$m was done by employing an argon-ion laser and optimizing the power density and exposure time of the laser. The exposure time was controlled by an electronic shutter. Uniform annealing over an area of 2 mm$\times$2 mm was also achieved by scanning the argon-ion laser over the sample using a *X*-*Y* precision translator and optimizing the annealing power density and scan speed of the translator.

The Raman scattering experiments were performed on the annealed spots and areas of the *a*-Si:H samples fixed on the cold finger of a helium cryostat using silver paste, and the temperature was regulated down to 10 K from room temperature using a HELITRON closed-cycle liquid-He cryostat. The cryostat was evacuated to $1\times10^{-6}$ torr to avoid condensation of moisture on the sample at low temperatures. A microprocessor-based digital temperature controller was used to regulate the temperature with an accuracy of $\pm0.3$ K. The temperature of the sample was measured accurately by mounting a chromel vs gold thermocouple on the cold finger. The monochromator was calibrated using the strong plasma lines of the argon-ion laser. Each experiment was carried out three times, and the average values of the peak position and peak width were taken to avoid random errors. The excitation power of the argon-ion laser was kept low to avoid local heating of the sample. The slit width of the monochromator was set to 100 $\mu$m. The instrumental resolution at this slit width is about 1 cm$^{-1}$. Raman experiments on the annealed samples were performed at seven different temperatures varying between 20 and 300 K.

## III. EXPERIMENTAL RESULTS AND DISCUSSION

### A. Size dependence at room temperature

Relaxation of the selection rules due to phonon localization inside the nanocrystal results in softening and broadening of the first-order phonon in Raman scattering. It is possible to make an estimate of the average dimension of nanocrystals by comparing the experimental line shape of the first-order Raman spectrum with theoretical ones using the simple phenomenological model of Richter *et al.*[5] and Campbell and Fauchet.[6]

We have analyzed our experimental results using a Gaussian weighting function in this model with a value of $\exp(-4\pi^2)$ at the boundary of the crystallites. This choice corresponds to rigid confinement of the phonons in the nanocrystal so that the amplitude vanishes at the boundary.

The first-order Raman spectrum is therefore given by

$$I(\omega)=\int_0^1 \frac{\exp(-q^2L^2/4a^2)}{[\omega-\omega(q)]^2+(\Gamma_0/2)^2}\,d^3q. \tag{1}$$

Here $q$ is expressed in units of $2\pi/a$, $a$ is the lattice constant (5.430 Å) of silicon, and $\Gamma_0$ is the linewidth of the silicon LO phonon in C-Si bulk ($\sim$4 cm$^{-1}$ including instrumental contributions), and $L$ is the average dimension. The dispersion $\omega(q)$ of the LO phonon is given by the relation[18]

$$\omega^2(q)=A+B\cos(\pi q/2), \tag{2}$$

where $A=1.714\times10^5$ cm$^{-2}$ and $B=1.000\times10^5$ cm$^{-2}$. A proper line-shape fitting of the experimental results is needed for evaluation of the average dimension of nanocrystals correctly. However, several factors such as the interfacial strain, amorphous contribution, size distribution of nanocrystals, and shape of nanocrystals influence the line shape and complicate the theory. Nanocrystalline silicon samples produced by cw laser annealing, in the present study, for example, show an appreciable contribution from amorphous silicon at low values of the power density and exposure time of the annealing laser beam. A fitting procedure[19] was used to separate the broad overlapping amorphous Raman peak from the nanocrystalline peak. With the increase in the power density and exposure time of the laser, however, the amorphous component becomes negligible and does not influence the full width at half maximum (FWHM) of the nanocrystallinelike peak. Also, with the increase in the power density and exposure time of the laser, the nanocrystallinelike mode shifts to higher frequency and becomes narrower and more symmetric, suggesting an increase in the dimension of nanocrystals.

Figure 1 shows the relationship between the peak shift and peak width in nanocrystalline silicon. The solid line shows the theoretical curve calculated using Eqs. (1) and (2). The experimental values seem to agree with the theoretical curve fairly well except at higher values of $L$, which could be due to the presence of strain in the annealed films.

The difference in the thermal expansion coefficient of quartz and silicon leads to tensile stress across the interface between the substrate and thin film when the films are cooled after laser irradiation during the annealing process. Tensile stress in the film leads to a softening of the Raman phonon mode. In general, strain in crystalline silicon causes the threefold-degenerate zone-center optical phonon to shift and split.[20] For uniaxial stress, it is possible to separate the shift coming from the hydrostatic component of the strain from the splitting. To do this, one must know the orientation of the crystal and stress and adjust the incident polarization and analyze the scattered light accordingly. The orientation of our crystallites was not determined in the present study, and

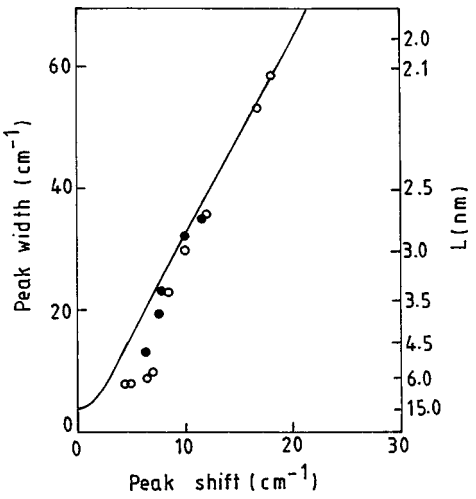


FIG. 1. Variation of peak shift and peak width of the first-order Raman line of nanocrystals produced by cw laser annealing of a 1100-Å-thick *a*-Si:H film. The open circles correspond to various annealing power densities and the solid circles to various annealing exposure times. The solid line is the theoretical result with a Gaussian weighting function. The right ordinate shows the corresponding dimensions $L$ in nm.

thus it is assumed that the observed shift is due to the hydrostatic component of the strain. Furthermore, a slight broadening of the Raman line is also observed due to the presence of stress, but the line shape is always symmetrical.[21] This is in sharp contradistinction to the effect in nanocrystals when the wave-vector nonconservation rule leads to phonon softening and line broadening of the Raman spectrum, but the line shapes are highly asymmetric.

A rough estimate of the phonon softening due to tensile strain can be made as follows. The maximum volume change[22] due to hydrostatic strain when a silicon film on a quartz substrate is cooled from its melting temperature to ambient is $6\times10^{-3}$. Given the fact that the Gruneisen parameter for silicon is 0.91, this corresponds to a wave-number shift of 2.8 cm$^{-1}$. So this is qualitatively consistent with the deviation of the observed peak shifts from those expected theoretically for the larger nanocrystals given in Fig. 1. This deviation varies between 0.4 and 4.0 cm$^{-1}$.

Therefore, there could be some additional stress inducing mechanisms within the film, resulting, for example, from the localized nature of the recrystallization process (e.g., involving spatially nonuniform expansion within the film). It is also found that, in general, with increasing power density and exposure time, the magnitude of the strain increases. This is expected, because a larger value of the strain will be there for samples annealed at higher temperatures. However, at very high power densities, the strain values are low. The growth of the nanocrystals is governed by a bulk-induced solid-phase crystallization process;[23] i.e., the nucleation of crystallites is initiated by a statistically random occurrence of nucleation sites in the bulk of the crystal. This could be due to melting of the film at these high power densities leading to an alteration of strain values.

A large distribution of nanocrystalline sizes also leads to a discrepancy between the expected theoretical and experimental line shapes. However, in this case there is a very large broadening and unusual asymmetricity of the spectra. A good fit of the experimental line shape is thus not obtained in the framework of the phonon confinement model. When one considers only the FWHM and peak position, the experimental points will lie towards the left of the theoretical line (refer to Fig. 1). In our case, however, the experimental points lie towards the right, i.e., the Raman lines, are narrower than expected theoretically. Further, a shifting the Raman lines towards higher frequency results in good agreement of the experimental and theoretical line shapes. The sign and magnitude of the shift agree to what one would expect from the existence of tensile strain between the film and quartz substrate. The existence of tensile strain is further confirmed by the fact that on increasing the annealing power density, the linewidth continues to decrease and the line shape becomes more symmetric, but the line center persists at the same position. The existence of a very broad distribution of nanocrystal sizes would have resulted in a broader and asymmetric line shape. The effect of strain is pronounced only for the larger crystals when the annealing power density is very high. The growth temperature is higher in this case, and thus the phonon shift due to strain, which is proportional to the difference between the growth and ambient temperature, is also higher. For lower annealing power density, the growth temperature is less and consequently the strain effects are negligible. Therefore, it is clear from Fig. 1 that stable nanocrystals of dimensions in the range of 2–7 nm are produced by cw laser annealing of *a*-Si:H samples on quartz substrates with proper optimization of power density and exposure time.

### B. Temperature dependence

In bulk materials, both the line center and linewidth of optical phonons are found to vary with temperature. This temperature dependence can be attributed to anharmonic terms in the vibrational potential energy. Because of anharmonicity of the lattice forces, an optical mode can interchange energy with other lattice modes and in this way maintain thermal equilibrium. The principal anharmonic interactions are due to the cubic or quartic anharmonicities, resulting in the splitting of an optical phonon into two or three acoustic phonons, respectively.

According to Balkanski, Wallis, and Haro,[9] below the Debye temperature, the temperature dependence of the linewidth and line center of the one-phonon LO mode at the center of the Brillouin zone can be written as

$$\Gamma(T)=A\left[1+\frac{2}{(e^{x}-1)}\right] \tag{3}$$

and $\omega(T)=\omega_0+\Delta(T)$, where

$$\Delta(T)=C\left[1+\frac{2}{(e^{x}-1)}\right], \tag{4}$$

where $x=\hbar\omega_0/2k_BT$, $A$ and $C$ are anharmonic constants, and $\omega_0$ is the intrinsic frequency of LO phonon.

In nanocrystals, finite-size effects have also to be taken into account, but unfortunately, no theory of anharmonic effects exists for this. We therefore assume that the temperature dependence of the phonon structures in nanocrystals is the same as that of phonons in the bulk and that the equa-

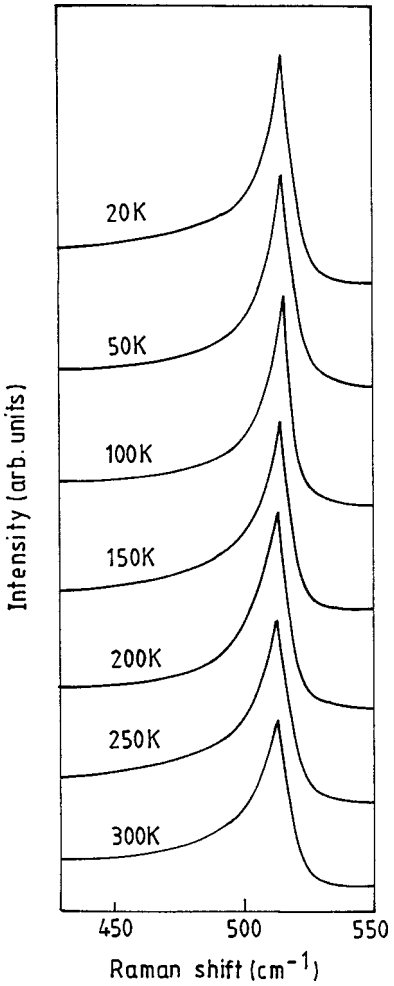


FIG. 2. Temperature dependence of the first-order phonon of nanocrystals of 5.1 nm average size.

tions given previously are valid. Furthermore, we assume that disorder and boundary scattering in finite-size crystals lead to temperature-insensitive additional broadening of the phonon lines.[24] Therefore, Eq. (3) becomes

$$\Gamma(T)=\Gamma_1+A\left[1+\frac{2}{(e^x-1)}\right]=\Gamma_1+\Gamma_0(T), \qquad (5)$$

where $\Gamma_1$ is the additional broadening due to the finite-size effects and $\Gamma_0(T)$ is the temperature-dependent intrinsic

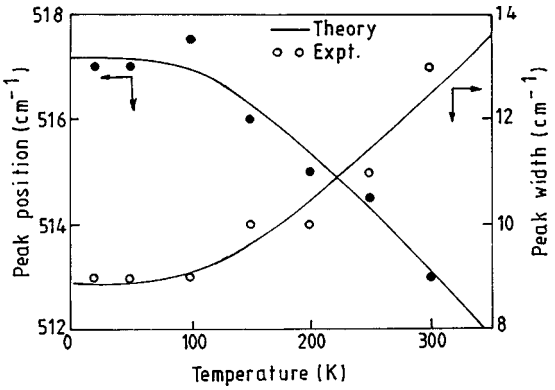


FIG. 3. Variation of peak position and peak width with temperature for nanocrystals of average size 5.1 nm.

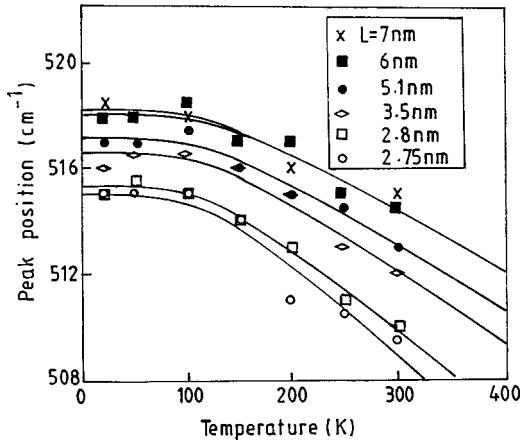


FIG. 4. Variation of peak position with temperature for nanocrystals of different dimensions. Solid lines are theoretical fits using Eq. (4). The various symbols shown correspond to experimental points.

width of the first-order phonon. Equation (5) can be used to explain the variation of the linewidth of the Raman line with temperature in nanocrystals, provided the value of $\omega_0$ is properly chosen to include the additional shift of the Raman line due to the confinement of phonons.

Figure 2 shows the first-order mode of nanocrystals of average dimensions 5.1 nm at different temperatures. The average experimental values for the linewidth and line center have been plotted in Fig. 3. Equations (4) and (5) have been used to fit the experimental data by suitably choosing the constants $\omega_0$, $A$, $C$, and $\Gamma_1$, and the agreement between the theoretical curve and experimental points is found to be quite good. Figure 3 typically shows that the linewidth increases, whereas the line center shifts towards lower frequency with increasing temperature. The same trend is observed for nanocrystals of other dimensions. Figures 4 and 5 show the variation of line center and linewidths with temperature for nanocrystals of different average dimensions. The solid lines give the theoretical fits to the experimental points. The variation of the absolute value of $C$ with nanocrystal size is given in Fig. 6. The anharmonic constant $A$ and temperature-

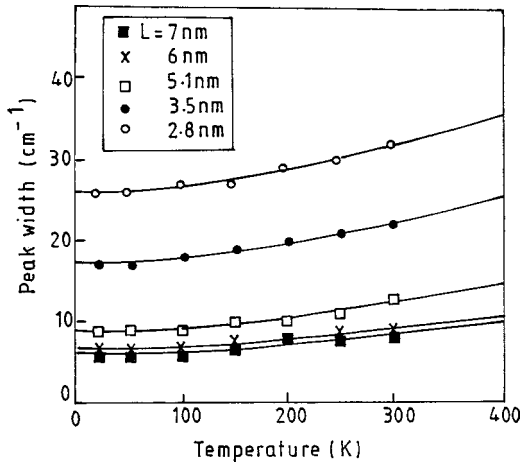


FIG. 5. Variation of peak width with temperature for nanocrystals of different dimensions. Solid lines are theoretical fits using Eq. (5). The various symbols shown correspond to experimental points.

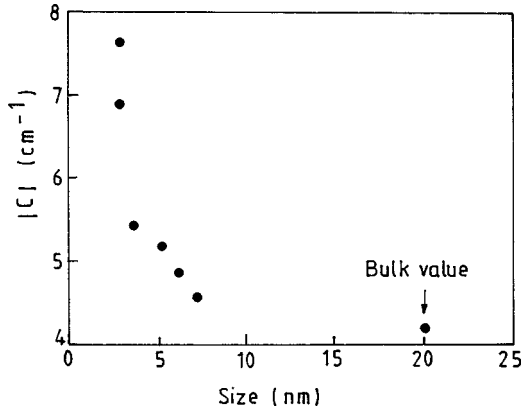


FIG. 6. Variation of the anharmonic constant $|C|$ with nanocrystal size. The bulk value is also shown.

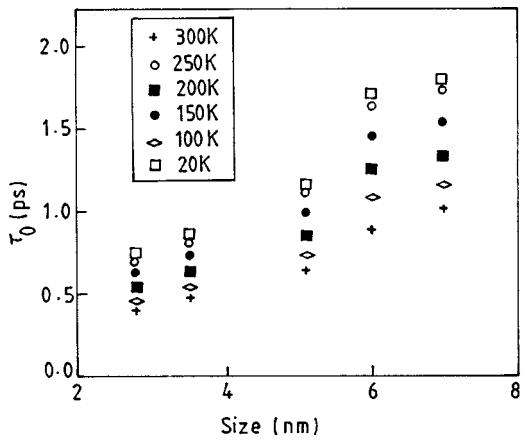


FIG. 8. Variation of the intrinsic lifetime $\tau_0$ with nanocrystal size at different temperatures.

independent broadening parameter due to finite-size effects, $\Gamma_1$, as a function of nanocrystal size are given in Fig. 7. The corresponding values for bulk silicon are also indicated in the figures. All of these parameters, $C$, $A$, and $\Gamma_1$, are found to increase rapidly with a decrease in the dimension of the nanocrystals. Further, $\Gamma_1$ is found to increase more rapidly than $A$ with decreasing size of nanocrystals. The rapid increase of the constants $A$, $C$, and $\Gamma_1$ with decreasing nanocrystal size and the fact that these values are much greater than the corresponding values in bulk silicon imply that the anharmonic effects are more important in nanocrystals than in bulk silicon. The constant $\omega_0$ seems to be independent of the size of nanocrystals.

The linewidth is reciprocally related to the lifetime of the decay process, and so the constant $A$ can be related to the phonon lifetime. The thermal interaction increases with increasing temperature, decreasing the phonon mean free path with a consequent decrease in the decay lifetime. Consequently, the linewidth increases at high temperatures. Further, the inherent boundary scattering in nanocrystals is expected to further decrease the decay times.

Hart *et al.*[11] predicted a mean phonon lifetime of $2.5 \times 10^{-12}$ s corresponding to a zero-temperature linewidth with a value of $A = 2.1\,\mathrm{cm}^{-1}$ for bulk silicon. However, for silicon nanocrystals, there are two different contributions to the first-order phonon peak widths: the temperature-independent width $\Gamma_1$ due to finite-size effects and the temperature-dependent width $\Gamma_0$ due to anharmonicity effects. Two different decay times $\tau_0$ and $\tau_1$ are therefore defined, related inversely to $\Gamma_0(T)$ and $\Gamma_1$, respectively. The phonon lifetimes were calculated using the relation $\tau = \hbar/2\pi c\Gamma$, where $c$ is velocity of light and $\Gamma$ is the linewidth. The variation $\tau_0$ with temperature and dimension is plotted in Fig. 8. The intrinsic lifetime $\tau_0$ is related to anharmonic effects, and it is observed that $\tau_0$ increases with a decrease in temperature and the rate of change is higher for larger nanocrystals. It is also clear that $\tau_0$ decreases with decreasing size. For instance, typical values of $\tau_0$ lie between 0.7 and 1.7 ps for nanocrystals of various sizes at low temperatures, while the value of $\tau_0$ for bulk silicon is 2.5 ps.

The phonon lifetime $\tau_1$, which is related to the temperature-independent broadening parameter $\Gamma_1$, also decreases with decreasing dimensions. The ratio $\tau_0/\tau_1$ has been plotted in Fig. 9 to compare the two lifetimes. It is clear from Fig. 9 that $\tau_0/\tau_1$ is greater than 1 for nanocrystals of dimension less than 4 nm and it is less than 1 for larger nanocrystals. This implies that phonon decay due to finite-size effects dominates for smaller nanocrystals, while the decay of phonons is mainly due to anharmonic effects for larger nanocrystals. The resultant phonon decay in nanostructures is thus dominated by both $\tau_0$ and $\tau_1$ and is found to be faster than that in the bulk.

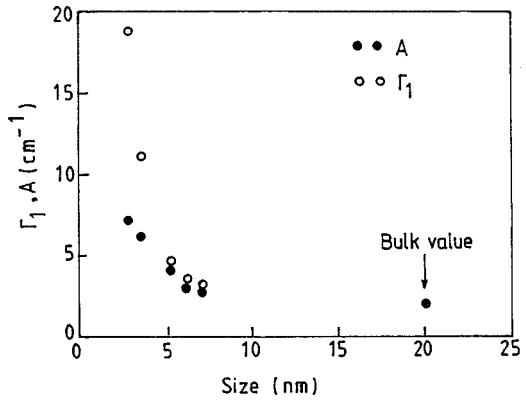


FIG. 7. Variation of the anharmonic constant $A$ and temperature-independent broadening $\Gamma_1$ with nanocrystal size. The corresponding values for the bulk are also shown.

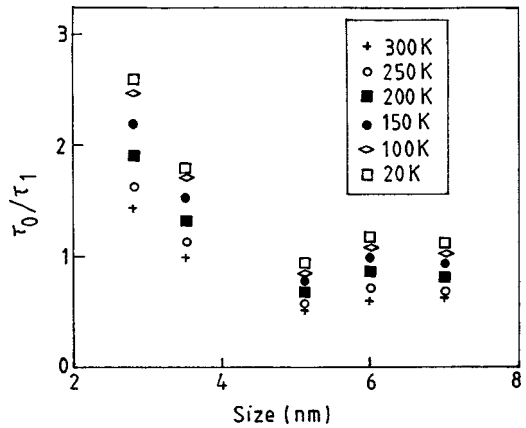


FIG. 9. Variation of $\tau_0/\tau_1$ with nanocrystal size at different temperatures.

## IV. CONCLUSION

In conclusion, nanocrystals in the range 2–7 nm have been made by cw laser annealing of *a*-Si:H films. The average size of nanocrystals was calculated by a detailed lineshape analysis of the Raman scattering using a phenomenological model and taking into account the contribution of interfacial strains and amorphous background. A comparative temperature-dependent Raman study indicated that the anharmonic constants related to the peak widths and peak positions are higher in nanocrystals than in the bulk, implying a greater degree of anharmonicity in nanocrystals. The anharmonic constants were found to depend on the nanocrystal size and increased asymptotically with a decrease in dimensions. Two different contributions to the phonon decay times $\tau_0$ and $\tau_1$ related to the temperature-sensitive intrinsic width $\Gamma_0$ and the temperature-insensitive disorder and the finite-boundary-related width $\Gamma_1$ were observed. A thermal interaction at higher temperature decreases the inherent phonon decay time $\tau_0$. Both $\tau_0$ and $\tau_1$ are found to be sensitive to the nanocrystal size and decrease rapidly with decreasing size, the change being faster for $\tau_1$. As expected, it is found that the phonons decay via the intrinsic path for larger crystals, while the decay at the finite boundary becomes more pronounced in smaller crystals.

*Present address: Department of Communications and Systems, University of Electro-communications, 1-5-1 Chofugaoka, Chofushi, Tokyo-182-8585, Japan.

[1] *Nanostructures and Mesoscopic Systems*, edited by M. Read and W. Kirk (Academic, San Diego, 1991).

[2] *Nanostructured Systems, Semiconductors and Semimetals*, edited by R. K. Williardson, A. C. Beer, and E. R. Weber (Academic, San Diego, 1992), Vol. 35.

[3] L. T. Canham, Appl. Phys. Lett. **57**, 1046 (1990).

[4] Y. Kanemitsu, T. Ogawa, K. Shiraishi, and K. Takeda, Phys. Rev. B **48**, 4883 (1993).

[5] H. Richter, Z. P. Wang, and L. Ley, Solid State Commun. **39**, 625 (1981).

[6] I. H. Campbell and P. M. Fauchet, Solid State Commun. **58**, 739 (1986).

[7] S. Das Sarma, in *Hot Carriers in Semiconductor Nanostructures: Physics and Applications*, edited by J. Shah (Academic, Boston, 1992), pp. 53–58.

[8] S. Das Sarma, V. B. Campos, M. A. Stroscio, and K. W. Kim, Semicond. Sci. Technol. **60**, 7 (1992).

[9] M. Balkanski, R. F. Wallis, and E. Haro, Phys. Rev. B **28**, 1928 (1983).

[10] P. G. Klemens, Phys. Rev. **148**, 845 (1966).

[11] T. R. Hart, R. L. Aggarwal, and Benjamin Lax, Phys. Rev. B **1**, 638 (1970).

[12] E. Bustarret, M. A. Hachicha, and M. Brunel, Appl. Phys. Lett. **52**, 1675 (1988).

[13] Z. Sui, P. P. Leong, I. P. Herman, G. S. Higashi, and H. Temkin, Appl. Phys. Lett. **60**, 2086 (1992).

[14] M. Fujii, Y. Kanzawa, S. Hayashi, and K. Yamamoto, Phys. Rev. B **54**, R8373 (1996).

[15] K. K. Tiong, P. M. Amritharaj, F. H. Pollak, and D. E. Aspnes, Appl. Phys. Lett. **44**, 122 (1984).

[16] M. Holtz, R. Zallen, O. Brafman, and S. Matteson, Phys. Rev. B **37**, 4609 (1988).

[17] A. Tanaka, S. Onari, and T. Arai, Phys. Rev. B **45**, 6587 (1992).

[18] Y. Kanemitsu, H. Uto, Y. Masumoto, T. Matsumoto, T. Futagi, and H. Mimura, Phys. Rev. B **48**, 2827 (1993).

[19] G. Mariotto, F. Ziglio, and F. L. Freire, Jr., J. Non-Cryst. Solids **192&193**, 253 (1995).

[20] E. Annastassakis, A. Pinczuk, E. Burstein, F. H. Pollak, and M. Cardona, Solid State Commun. **8**, 133 (1970).

[21] D. J. Olego, H. Baumgart, and G. K. Celler, Appl. Phys. Lett. **52**, 483 (1988).

[22] S. A. Lyon, R. J. Nemanich, N. M. Johnson, and D. K. Biegelsen, Appl. Phys. Lett. **40**, 316 (1982).

[23] K. Zellama, P. Germain, S. Squelard, J. C. Bourgoin, and P. A. Thomas, J. Appl. Phys. **50**, 6995 (1979).

[24] B. Kh. Bairamov, Yu. E. Kitaev, V. K. Negoduiko, and Z. M. Khashkhozhev, Fiz. Tverd. Tela (Leningrad) **16**, 2036 (1974) [Sov. Phys. Solid State **16**, 1323 (1975)].